An IEEE 802.11p Empirical Performance Model for Cooperative Systems Applications

Sébastien Demmel, Grégoire Larue, Dominique Gruyer and Andry Rakotonirainy

Abstract— IEEE 802.11p is the new standard for Inter-Vehicular Communications (IVC) using the 5.9 GHz frequency band, as part of the DSRC framework; it will enable applications based on Cooperative Systems. Simulation is widely used to estimate or verify the potential benefits of such cooperative applications, notably in terms of safety for the drivers. We have developed a performance model for 802.11p that can be used by simulations of cooperative applications (e.g. collision avoidance) without requiring intricate models of the whole IVC stack. Instead, it provide a a straightforward yet realistic modelisation of IVC performance. Our model uses data from extensive field trials to infer the correlation between speed, distance and performance metrics such as maximum range, latency and frame loss. Then, we improve this model to limit the number of profiles that have to be generated when there are more than a few couples of emitter-receptor in a given location. Our model generates realistic performance for rural or suburban environments among small groups of IVC-equipped vehicles and road side units.

I. INTRODUCTION

Cooperative applications based on the usage of Inter-Vehicular Communications (IVC) are a very popular research topic, with many potential benefits to be found in safety, entertainment and comfort [1], [2], [3]. In order to evaluate these potential benefits, the main avenue of research has been simulation, with for example studies looking at the effectiveness of Emergency Electronic Brake Light (EEBL) [4], [5], Cooperative Collision Warning (CCW) [6], or variable speed limits [7]. Several factors are required in those simulations in order to accurately reproduce the performance of future applications, including but not limited to realistic environment and kinematic models, plausible driver behaviour simulations, and accurate IVC performance models. In this paper, we shall focus on that latter item.

In advanced higher-level simulations, the intricate simulation of the whole IVC network performance, including the various layers of the OSI model, is possible. Software such as the NS-x family or OMNeT++ can be used to simulated IVC networks, with a complex topology; using such an approach allows studying the dissemination of information in vehicular network to a large scale. At the lowest level, those software use physical propagation models that are used to infer the performance of connection between vehicles and roadside

units. However, there are few physical models based on empirical data. We have previously shown that the theoretical and actual performance of IEEE 802.11p are likely to diverge considerably [8]. In order to account for those variations, especially to verify they do no hinder the expected benefits of cooperative applications, models constructed from empirical data are necessary. Recent developments have shown interesting approaches for NS-2/3, such as using a Two-Ray Interference model for line-of-sight (LoS) conditions [9], or improving non-LoS conditions [10], [11]. As we mentioned earlier, these models focus on simulating the received power given a certain distance; performance indicators such as delivery ratio or range can be computed from those lower level simulations. However, our experimental data suggest that these models are not capable of representing all the performance variations that we measured on the road. Another issue is that one needs to link the network simulator with the application simulator, which can prove to be a time-consuming task. Such framework already exist for traffic simulation, such as the VEINS software suite[1], but not for detailed microscopic simulations. In most cases, a simple yet realistic model of IVC performance would provide satisfying performance.

Our goal is to develop a model to simulate performance indicators (frame loss, latency) based on empirical data and that can be implemented directly inside the software used to simulate cooperative applications (in our case, the SiVIC-RTMaps framework [12], [13]). Such a model would bridge a gap between physical layer and network models by providing a focus on some simple, yet central, performance indicators for IEEE 802.11p in small-to-medium-sized networks where no routing (or complex topology) is required; it is entirely focused on delivering realistic performance indicators to upper-layer cooperative applications simulations.

The remainder of this paper is organised as follows: Section II presents the construction of our model, starting with a short summary of our experimental results (II-A), then details the frame loss model (II-B), the latency model (II-C), and limitations (II-D). Section III then outlines improvements that are made on the model based on further data collection. Eventually, we offer conclusions and perspective on future works in Section IV.

[1]veins.car2x.org

II. A PERFORMANCE-ORIENTED IEEE 802.11P MODEL

A. Summary of experimental results

In order to develop an empirical performance model of IEEE 802.11p, we required a large amount of data collected with IVC real devices on the road, or at least in an environment that is a relatively close approximation of the road. The chosen test location was the test tracks of Satory (near Versailles, France), that can stand in for a suburban or rural environment. The experimental setup, scenarios, and detailed results can be found in [8], [14]. For the remainder of this section, we will give a brief overview of our previous findings.

The data collection was shaped toward three metrics: the maximum range, frame loss and latency. Range and frame loss are related, since the maximum range is equal to the point where frame loss remains at 100% for good (a brief interruption of signal with a frame loss of 100% does not mean that we have reached the maximum range yet).

Given our setting, the maximum range measured was 1,397 metres, in line with the standard. However, we found that the maximum range was strongly correlated to the relative speed between the emitter and receptor, and shrunk considerably while the speed increased. At 30 km/h the average maximum range is about 900 metres, while at 130 km/h the average maximum range has decreased to 350 metres. Initial measurements suggested an important difference arising from the direction of driving: the maximum range would shift by hundreds of metres depending whether the vehicle was driving away or toward the RSU. However, further investigations shown that this effect was merely resulting from the combination of antennas' inhomogeneities and some amplificatory effect by the vehicle's body shape (for more details, see [8], section IV-A). When properly controlled for those latter effects, there was no significant difference due to the direction of movement.

Frame loss measurements showed a consistent behaviour: the frame loss would remain low for a large part of the range before rising relatively sharply over the last 200 to 300 metres. It was found to sometimes fluctuate in a seemingly random fashion. We noted a consistent peak around 120 metres from the emitter, which can be explained by two-ray ground reflection interferences related to the setup's geometry [15], [16], especially the antenna's height above ground. In other locations factors in the environment compounded to focus the emitter's signal and decreasing frame loss where it was otherwise high or previously increasing.

Measurements in a clean network situation (i.e. just the 2 vehicular IVC devices together) showed that the latency did not depend on range and relative speed, remaining under 5 milliseconds in 99.47% of cases for a BSM-like message. In more crowded network conditions, with up to 6 IVC devices competing for the medium, we found that the average latency did not vary much but there was an increased spread, with larger latency becoming more common because of the competition between the IVC devices. This result was expected, and we quantified the average latencies and their spread (through the standard deviation) for different frame sizes, from 84 bytes to 1 kilobytes.

B. Frame loss model

After having analysed the experimental data, as summarised above, we are now looking into creating a model that studies the correlation between speed, distance and performance for the frame loss metric. Section II-C will show that there is no need for this approach when considering latency.

The frame loss model is based on the concept of *profiles*. A profile represents a single uninterrupted, temporally consistent connection between two IVC devices and is used to determine the frame loss probability at any given distance, as long as they are within range of each other. Any given profile will be different from the others, but when averaging them all we can reproduce the averaged results of the experimental measurements; this means that individual profiles might introduce some "novelty" in terms of performance compared to the measurements, but they will always tend toward those latter. Some profiles will closely match individual measurements laps. Each individual profile represents a set of specific conditions that could be found on the road; for example, a profile can represent realistically the conditions on a sunny or on a rainy day.

1) Profiles: Let us have τ a frame loss profile (see Fig. 1) defined by Eq. (1) where d is the distance between the emitter and receptor and $A, B, \ldots F$ are parameters estimated from empirical data.

$$\tau = \max \left[A . \exp^{B.(d-C)^2} ; \min \left(\max \left[D.d + E ; F \right] ; 1 \right) \right] \tag{1}$$

τ can be decomposed into two terms. The first term $A . \exp^{B.(d-C)^2}$ represents the frame loss area corresponding to the strongest ground reflection interferences, centred at distance C. At this point the ground-reflected signal is strong enough to cancel out a large proportion of the incoming direct signal's energy, pushing a proportion of frames under the chipset reception's threshold; the frame loss corresponding to this proportion is represented by A. The bell curve's width is proportional to B; note that B is always negative. The model assumes that no counter-measure is applied to reduce the frame loss induced by interferences at C; it also assumes the vehicles' environement has the appropriate geometry. Overall, our model will over-estimate the error due to ground reflection, rather than under-estimate it.

The second term $D.d + E$ is a linear regression where τ is modelled linearly as a function of distance d and parameters D and E. This term represents the progressive increase of frame loss as received signal strength decrease.

The increase starts from a non-zero frame loss ratio value given by parameter F, which represent the average of small perturbations measured within range. Typically, F will be low (less than 5%). D and E by themselves have no direct physical meaning; however, there are two meaningful ratios: ratio $\frac{F-E}{D}$ gives the distance at which frame loss starts to increase from the plateau at F; ratio $\frac{1-E}{D}$ expresses the distance at which frame loss reaches 100% (or in other words where $\tau = 1$), hence the maximum range.

2) Classes & parameters estimation: Based on experimental data, we created four classes which are classified according to the relative speed between the emitter and receptor. Each class has its own set of parameters values. The classes are [0;40], [40;60] [60;100], and [100;160] km/h (based on the speeds found on different types of road: urban, main road, etc.).

Parameters $A, B, \ldots F$ excluding E are estimated on the experimental data using the Levenberg-Marquardt algorithm for non-linear least squares [17]. Experimental data show that D and E are linearly correlated through the Generalised Linear Model regression shown in Eq. (2). Indeed, the distance required to increase from $\tau = 0\%$ to $\tau = 100\%$ (i.e. the profile's slope) is relatively consistent over the dataset so as a result only D needs to be estimated to obtain both D and E, with $E = f(D)$ according to Eq. (2). The linear regression coefficients $\{\alpha, \beta\}$ are themselves estimated from experimental data and can be further divided into sub-classes for an improved fidelity to experimental data, if required. No statistically significant correlation was found for any other parameters.

$$E = \alpha D + \beta + e \quad e \rightsquigarrow \mathcal{N}(0, \sigma) \tag{2}$$

Then, a non-parametric probability density estimate is computed to extract the continuous distribution $\mathbf{A}, \mathbf{B}, \ldots \mathbf{F}$ for each parameter; this is achieved with a Gaussian kernel smoothing method. Changing the parameters of the Gaussian kernel smoothing allows generating distributions for the model's parameters that either closely reproduce experimental data or, on the other hand, that allow non-measured but plausible profiles.

The last step consists in transforming $\mathbf{A}, \mathbf{B}, \ldots \mathbf{F}$ to cumulative distribution functions $G_{\mathbf{x}}$ where $\mathbf{x} \in \{\mathbf{A}, \mathbf{B}, \ldots \mathbf{F}\}$, excluding $\mathbf{E}$. These cumulative distributions can then be used to generate the parameters' values with an inverse transform sampling method when generating a profile (see next subsection).

3) Generating the profiles: When generating any new τ, the parameters' distributions (specifically cumulative distribution $G_{\mathbf{A}}, G_{\mathbf{B}}, \ldots, G_{\mathbf{F}}$) are used to generate realistic random values for $A, B, \ldots F$, using the following pseudo-algorithm:

1) For each $x \in \{A, B, \ldots F\}$ excluding E // x is a parameter and $\mathbf{x}$ its distribution
   a) $u \leftarrow \mathcal{U}(0,1)$ // a random number u is generated from the uniform distribution $\mathcal{U}(0,1)$
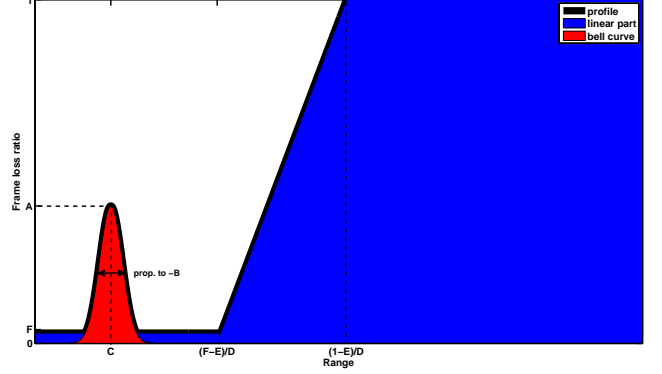

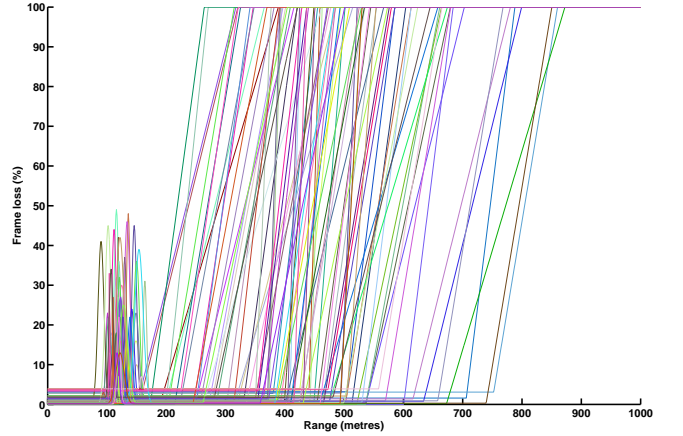Fig. 1: Decomposition of a frame loss profile τ, with its parameters

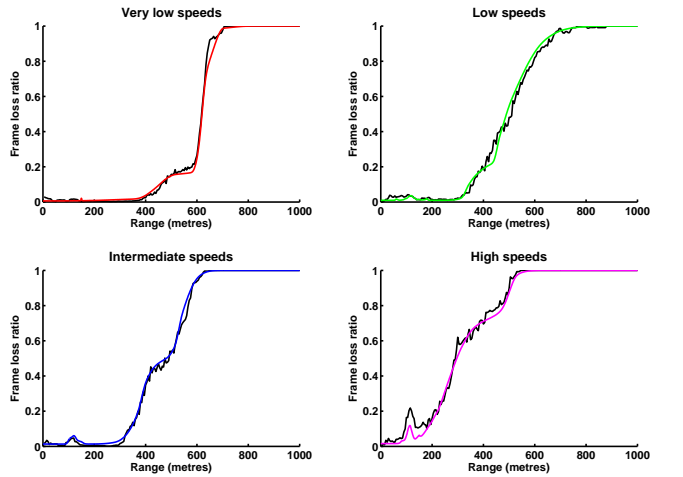Fig. 2: Generation of frame loss profiles for the [60;100] km/h class with 100 drawings of u

Fig. 3: Averages of 1,000 profiles for each of the four classes, compared to the measured averages (in black)

b) $x \leftarrow G_{\mathbf{x}}^{-1}(u)$ // a parameter receives the value from its inverse cumulative distribution

2) End For
3) $E \leftarrow \alpha D + \beta + e$ // E is obtained from the linear relationship that links it to D, where α and β are the regression coefficients based on experimental data, and e is a Gaussian noise centred at 0 and with standard deviation extracted from experimental data
4) $\tau = \max\left[A.\exp^{B.(d-C)^2}; \min\left(\max\left[D.d + E; F\right]; 1\right)\right]$ // Once each parameter has been assigned a value, τ can be processed from the values with Eq. (1)

In Fig. 2 we show the results of the generation of a hundred profile for the $[60; 100]$ class ("intermediate speeds"), that is 100 drawings of u in total; it illustrate the large variability that our model can represent while still remaining plausible and representative to the experimental data on average. Ground-reflection interferences remain concentrated around the 120 metres mark, and the final total range varies from 900 metres at best, to 250 metres at worst. Note the consistency of the rising part's slope, which reproduce well the behaviour found with experimental data, even considering the large variability of $\frac{F-E}{D}$ i.e. the point where the slope starts.

If we average all those profiles, the result will closely match the average frame loss measured on the tracks. This is illustrated in Fig. 3 for all the classes, considering 1,000 profiles for each, with distributions that are set to the maximum fidelity to experimental data. Note that for the two lower speed classes ($[0;40]$, $[40;60]$ km/h), the peak associated with the ground reflection interferences is not visible *on average*; many individual profiles will still display some degree of interference, but they are dwarfed by a much larger set of profiles where interference is minimal. A similar phenomenon can be seen in Fig. 2, where the highest peaks reach 50% of loss, whereas the average is only 10% as per Fig. 3.

In a simulated environment, a profile can be generated each time a connection is established between 2 nodes (typically when they enter within a static maximum range threshold); one emitter can have several profiles active at the same time if it is connected with more than one receptor.

C. Latency model

The latency model is simpler than the frame loss model; indeed, experimental data show that the latency does not depend on the relative speed or distance, when considering small packets which are similar to BSM. Experimental data have further shown that when the activity on the wireless network increases, the average latency is constant (the geometric average remains the same, the arithmetic average increases) but there is an increased spread of recorded latencies, i.e. larger latencies are becoming more common (in the case of BSM sent at 40 Hz, the average latency was 5 milliseconds; the measured standard deviation was multiplied by 5, from 5.6 to 27.1 milliseconds, when comparing clean and noisy network conditions) We created our latency model to account for this effect as well as the message's size, which obviously increases the time necessary to transmit it.
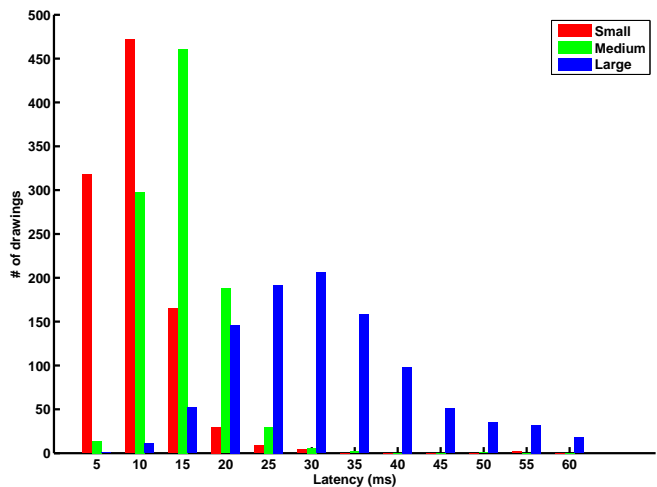

Fig. 4: Distribution of 1000 drawings of v for each of the three latency distributions

A simple algorithm is used to generate a latency d_i for each individual message $i \in \{1, \ldots n\}$, assuming there are n messages waiting to be exchanged at the present simulation time step. From the experimental data we obtained the cumulative distribution functions $G_{\mathbf{y}}$ where $\mathbf{y} \in \{\mathbf{L_S}, \mathbf{L_M}, \mathbf{L_L}\}$, with $\mathbf{L_S}, \mathbf{L_M}, \mathbf{L_L}$ continuous distributions built for three size of messages, respectively "small" i.e. <400 bytes, "medium" i.e. 400 to 800 bytes, and "large" i.e. >800 bytes. In effect, we have three classes of latency that depend on the size of the message. The BSM-like messages used for most of the data collection were 84 bytes, so it would fall in the "small" class, where the average measured latency was 1.5 milliseconds.

In order to simplify the model's implementation into a numerical simulation environment, the $G_{\mathbf{y}}$ distributions can be re-sampled to integer values of the simulation's timestep; for example, the simulation framework based on SiVIC that we used in previous research [18] has a timestep of 5 milliseconds. Given this latter information, the pseudo-algorithm used is the following:

1) For each messages i being sent at the present time step
   a) $y \leftarrow f(size[i])$ // the latency class is chosen among $\{\mathbf{L_S}, \mathbf{L_M}, \mathbf{L_L}\}$ through a function depending on the size of i
   b) $v \leftarrow \mathcal{U}(0,1)$ // a random number v is generated from the uniform distribution $\mathcal{U}(0,1)$
   c) $m_i \leftarrow G_{\mathbf{y}}^{-1}(v)$ // a multiplier m_i receives the value from the (re-sampled) inverse cumulative distribution
   d) $d_i = m_i \times 5ms$ // the delay d_i is computed
2) End For

Fig. 4 shows a sample distribution of delays generated for 1000 messages in each of the three classes.

D. Limitations

Our 802.11p performance model has a number of limitations. Those limitations arise both from the experimental conditions, that limits the amount of available data, and from the model's structure itself.

The model's main limitation is that it is representative of only a given set of environmental conditions and parameters, chiefly the location within which the data were collected. The Satory tracks are a good stand-in for rural or low-density suburban environments, either for a main road or a freeway, so the model will perform the most realistically within such environments. However, it cannot be used for an urban simulation, as it does not account for the effects of urban canyons such as increased multi-path, scattering, line of sight disruptions or possible focusing, as well as the presence of many vehicles.

Because the meteorological conditions were not precisely recorded during data collection, the impact of weather on performance could not be assessed. As a result, if we consider two vehicles that need a connection to a same roadside unit, the first generated profile might represent conditions measured during a dry and sunny day whereas the second profile could represent those of a humid overcast day. While we have been able to reconstruct the overall meteorological conditions during each day of the data collection, they were not varied enough to create a full spectrum of weather-based sub-classes for the parameters.

A further limitation is with the latency model, which is fairly simple. It does not take into account non-direct routing and considers only frames up to 1 kB (that can typically be transmitted as a single packet without fragmentation). Similarly with other performance indicator, this latency model would not be applicable to a situation with many IVC-equipped vehicles and/or complex network usage.

III. IMPROVEMENTS

A. Goal

Further than the aforementioned issue of meteorological conditions, the present model allows for two neighbouring nodes to have vastly diverging performance when connecting to a third same node, even if their profiles are generated from the same speed class. This can be illustrated with Fig. 2. Even though the average maximum range in the [60;100] km/h class is about 600 metres, we can see that for those 100 drawings of u, the maximum range actually varied from 265 to 873 metres. Even it not particularly likely, it is possible that those two bounds are picked up when creating the profile for two neighbouring nodes. Even within those extreme bounds, two neighbouring nodes could still have variations of maximum range of hundreds of metres. This might lead to one node being able to connect to the third one, while the other cannot.

A priori, this behaviour is very unrealistic. Indeed, although performance can vary quickly due to subtle environmental influences (a typical example is two-ray ground interference), we expect that two close IVC devices using similar hardware should have similar performance. For example, two vehicles following each other on a freeway would be able to connect

with similar efficiency (or lack thereof) to a RSU that broadcasts speed limit and traffic information.

As such, our goal is to experimentally verify whether this is the case and to adapt the model. If we can verify that a group of vehicles that connect to a RSU will exhibit similar performance, we can then generate a single profile for this group, instead of one profile for each vehicle. By doing so, we can reduce our model computational load, but more importantly make it far more realistic. Additional data collection will also help determining an adequate threshold for a profile's validity duration. Indeed, given a static geometry, a RSU that connects to passing vehicles might not need to generate new profiles each time a new vehicles enter its range every few minutes. Assuming similar hardware and vehicles, the environmental conditions might not change quickly enough for two profiles 5 minutes apart to be different, allowing re-using one profile more than once.

B. Experimental setup

For this test, we use a mobile emitter and two static receptors located 25 metres apart; we were forced to use this "reversed" configuration for logistical reasons. The distance between the two static receptors, 25 metres, is chosen for two reasons. Firstly, they are not too close; one would expect that there would not be much difference if the receptors are located one metre apart (this would be more relevant to a single vehicle with multiple antennas). Secondly, they are not too far apart either. Larger distance, over 50 metres, would defeat the purpose of studying the correlation introduced by close proximity. 25 metres is a good compromise considering the changes in relative distance that two vehicles can exhibit when driving together.

The mobile emitter is the Clio 3, and the static receptors are two RSU built from the same hardware used in previous tests [8], [14]. The effect of hardware, especially antennas, inhomogeneities is minimised by careful placement: the maximum gain regions of each antenna are placed so that they will face each other when the vehicle is driving toward the two receptors. As such, we expect that the range will be higher when moving toward the RSUs than when driving away.

This time, the measurements are performed on Satory's road track "la routière", with the RSUs placed near the centre of the 1.1-kilometres-long straight southern section of the track. The track's surroundings are similar to those of the speed track used in earlier experiments. The data collection was done during a single day in December 2012, with cold and overcast weather conditions.

C. Results & modelisation

In order to study the performance of nearby IVC devices, we consider the following indicators:

1) the distance at which frame loss starts to increase (the point described by $\frac{F-E}{D}$ in the model)

2) the distance required to reach 100% frame loss from the previous point (i.e. $\frac{1-E}{D}$)

We created Generalised Linear Models (GLM) for those indicators, using the experimental data. For both of these indicators, we will be looking at three possible effects that could influence them:

1) the receiving IVC device; hardware inhomogeneities might affect the performance as in our previous data collection.
2) the direction of travel.
3) the timing; timing is expressed in terms of "lap" around the track, and considered a factor in the GLM rather than a time value *per se*, this is done because we have no a priori assumption on the relationship between the conditions that existed in each consecutive lap.

Let us have the two RSUs be named A and B, and "closing" referring to parts of the laps when the vehicle is driving toward the RSUs, and "away" referring to the parts of the laps when the vehicle is driving away from the RSUs.

At first, we analysis the distance at which frame loss starts to increase from its plateau at low values; see Table Ia. Note that during a closing part, this distance corresponds to the point when the frame loss stops *decreasing* and reach its stable low-plateau value; as shown from our previous data, the driving direction's behaviour are symmetrical.

We consider the first lap and receiver A as references; data shows that lap #2, #4 and #7 (on a total of 9 here) are similar to the first one, yielding an average point $\frac{F-E}{D}$ at 304 metres for the away direction. When inverting the driving direction, the closing point $\frac{F-E}{D}$ was located 133 metres further for A, and 112 metres further for B. This confirms our previous expectations based on the antennas' relative orientations, as mentioned in III-B.

In the closing direction, A sees its frame loss increase 47 metre before B, whereas B sees its frame loss increase 62 metres before A in the away direction. 25 metres are easily explained by the distance between A and B , while the remaining difference probably arise from a combination of antenna effects, vehicle's body shape and slight geometrical effects.

While differences were observed between receivers, the overall frame loss trend for both receivers are similar for each lap. Half of the observed difference can be explained by the 25 meters separation between the receivers. The remaining difference (37 m) represents approximately a 10% difference (relative to the intercept) between the two receivers, and therefore the same profile can be used for two receptors located within a short distance, during the same lap.

Then, we use the second indicator (the distance to reach maximum range $\tau = 1$ from point $\frac{1-E}{D}$) to verify whether a same profile can be used over a longer period of time; in our setting, over several consecutive laps. Further confirmation that a same profile can be used for nearby receptors should also be obtained from this indicator. Data are shown in Table Ib.

TABLE I: Factors analysis

Factors	Estimate	Std. error	t value	$P(>|t|)$	signif.
Intercept	303.5	9.81	30.936	$< 2E-16$	***
direction: closing	+133.5	13.88	9.619	$2.44E-09$	***
lap: #3	+56.3	18.26	3.083	0.00544	**
lap: #5	+49.3	18.26	2.703	0.01299	*
lap: #6	+65.9	18.26	3.613	0.00154	**
lap: #8	+43.5	18.26	2.385	0.02612	*
lap: #9	+65.9	18.26	3.610	0.00155	**
receiver: B	-62.5	10.89	-5.738	$9.02E-06$	***
closing & #3	-68.9	25.81	-2.669	0.01403	*
closing & #5	-49.9	25.81	-1.936	0.0658	.
closing & #6	-63.2	25.81	-2.448	0.02281	*
closing & #8	-44.9	25.81	-1.741	0.09561	.
closing & #9	-67.7	25.81	-2.621	0.01559	*
closing & B	+112.1	15.4	7.282	$2.71E-07$	***

(a) Point $\frac{F-E}{D}$ location and influencing factors

Factors	Estimate	Std. error	t value	$P(>|t|)$	signif.
Intercept	29.78	7.81	3.806	0.000706	***
lap: #1	+335.86	14.62	22.968	$< 2E-16$	***
lap: #4	+52.89	19.15	2.762	0.01002	*
lap: #7	+106.02	19.15	5.537	$6.4E-06$	***
away & #1	-327.32	17.48	-18.728	$< 2E-16$	***
away & #7	-99.63	24.72	-4.031	0.000387	***

(b) Distance to reach $\tau = 1$ and influencing factors

In most cases (only 3 laps are significantly different from the reference), it took only 30 metres for the frame loss to rise to 100%, for both A and B. However, data show large variations between some consecutive laps, up to several hundred metres from the average, as shown for example in Table Ib for laps 1, 4 and 7. Each lap follows the previous one by only a few minutes, so those results suggest it is not possible to re-use the same profile for a similar location at two consecutive timestamps. Note that while the performance can change dramatically, weather conditions did not appear to change much over the same time frame.

On the other hand, we note that the variations that are measured are always found to affect both RSUs in similar proportion. This provides further support to the use of a single profile when considering nearby vehicles connected to the same IVC device.

Taking the example of an RSU located by the side of a freeway and connecting to a continuous flow of incoming vehicles, our model would allow to generate a new profile for small groups of vehicles that enter the RSU range together. However, it would not allow to use a single profile for the whole simulation, i.e. all vehicles. Indeed, the time elapsed between two given groups of vehicles will, after some duration threshold, be too important for conditions to remain similar and justify keeping a single profile according to the previous analysis. Unfortunately, the present work does not allow setting any realistic value for said threshold.

IV. CONCLUSION AND FUTURE WORKS

In this paper, we presented a performance model for IEEE 802.11p-based IVC aimed at higher-level simulations of Co-

operative Systems applications such as Electronic Emergency Brake Light, Cooperative Collision Warning or Cooperative Autonomous Cruise Control. In such simulation, the intricate simulation of the IVC network performance is not necessary and might prove to use resources for little gains, thus a simple yet realistic model of IVC performance should be deployed instead.

Our model is based on the data collected during extensive field trials conducted over the Satory's test tracks (presented in a previous paper [8]), and focuses on three fundamental metrics: range, frame loss, and latency, using only the relative speed and distance as inputs. We use the *frame loss profile* concept: one profile provides a continuous frame loss probability over the whole range, for each connection established between two IVC devices, on-board or on the roadside. Each profile includes a loss peak representing Two-Ray ground interference, arising from the vehicle-RSU geometry, followed by a linear increase of loss over a given distance, until maximum range is reached. The profile's parameters are estimated from collected data to generate profiles that reproduces those data while still allowing enough variability for the generation of new plausible data. A simple latency model is proposed, accounting for the effects of increased network activity and size of the frame transmitted; this model also uses empirical data.

Then, we explore possible improvements in terms of computing performance, by looking into limiting the number of profiles that need to be generated inside a simulated environment. Using additional experimental data, we found that two nearby IVC devices (located within 25-30 metres-radius circle) can use the same profile to connect to a single other device. This would potentially allow to limit the number of connection that have to be simulated in a crowded road environment; indeed, otherwise if there are n active devices in the simulation, the maximum number of active connections would be $\frac{n(n-1)}{2}$. However, our data does not allow for the same profile to be re-used when considering a same IVC device pair but taken at two consecutive timestamps separated by a few minutes; our data suggest that variations in the communications' performance can be very large within only a few minutes, even though the weather remains similar.

Future work should concern the collection of more data covering a wider range of weather conditions, especially humidity. The data collection is planned to take place in Australia (in south-eastern Queensland) over the course of 2013, in order to maximise the chance of obtaining diverse conditions ranging from dry sunny days to wet colder ones, and all combinations in-between. We will also look into quantifying the performance difference that may arise from hardware inhomogeneities. This should allow a more realistic simulation of larger groups of IVC-equipped vehicles whose hardware's quality might vary depending on the vehicle's age and maintenance.

REFERENCES

[1] A. A. Carter, "The status of vehicle-to-vehicle communication as a means of improving crash prevention performance," National Highway Traffic Safety Administration, U. S. Department of Transportation, Tech. Rep. 05-0264, 2005.

[2] S. Yoshizu, H. Oguri, and T. Miyakosh, "Estimation of accident reduction effect of cooperative safety system using actual road test data," in *15th ITS World Congres*, 2008.

[3] S. Demmel, D. Gruyer, and A. Rakotonirainy, "V2v/v2i augmented maps : state-of-the-art and contribution to real-time crash risk assessment," in *20th Canadian Multidisciplinary Road Safety Conference*. Hilton Niagara Falls, Ontario: The Canadian Association of Road Safety Professionals, June 2010.

[4] B. Mourllion, "Extension d'un système de perception embarqué par communication. application à la diminution du risque routier." Ph.D. dissertation, Université Paris Sud (Orsay, Paris XI), 2006.

[5] A. Lambert, D. Gruyer, A. Busson, and H. M. Ali, "Usefulness of collision warning inter-vehicular system," *International Journal of Vehicle Safety*, vol. 5, no. 1, pp. 60–74, 2010.

[6] Y. Takatori and T. Hasegawa, "Performance evaluation of driving assistance systems in terms of the system diffusion ratio," in *IEEE Conference on Intelligent Transportation Systems*, 2005, pp. 338 –342.

[7] D. Gruyer, S. Glaser, B. Vanholme, and B. Monnier, "Simulation of automatic vehicle speed control by transponder-equipped infrastructure," in *9th International Conference on Intelligent Transport Systems Telecommunications*, October 2009, pp. 628–633.

[8] S. Demmel, A. Lambert, D. Gruyer, A. Rakotonirainy, and E. Monacelli, "Empirical IEEE 802.11p performances evaluation on test tracks," in *IEEE Intelligent Vehicles Symposium*, 2012, pp. 837–842.

[9] C. Sommer and F. Dressler, "Using the right two-ray model? a measurement based evaluation of PHY models in VANETs," in *17th ACM International Conference on Mobile Computing and Networking*. Las Vegas, NV: ACM, september 2011.

[10] C. Sommer, D. Eckhoff, R. German, and F. Dressler, "A computationally inexpensive empirical model of IEEE 802.11p radio shadowing in urban environments," in *Eighth International Conference on Wireless On-Demand Network Systems and Services*, january 2011, pp. 84 –90.

[11] T. Mangel, O. Klemp, and H. Hartenstein, "A validated 5.9 ghz non-line-of-sight path-loss and fading model for inter-vehicle communication," in *11th International Conference on ITS Telecommunications*, august 2011, pp. 75 –80.

[12] D. Gruyer, S. Glaser, and B. Monnier, "SiVIC, a virtual platform for ADAS and PADAS prototyping, test and evaluation," in *FISITA World Automotive Congress*, June 2010.

[13] D. Gruyer, S. Glaser, S. Pechberti, R. Gallen, and N. Hautiere, "Distributed simulation architecture for the design of cooperative ADAS," in *First International Symposium on Future Active Safety Technology toward zero-traffic-accident*, September 2011.

[14] S. Demmel, "Building an augmented map for road risk assessment," Ph.D. dissertation, Queensland University of Technology & Université de Versailles Saint-Quentin-en-Yvelines, 2013.

[15] P. Lacomme, *Air and Spaceborne Radar Systems: An Introduction*, ser. Press Monographs. William Andrew, 2001.

[16] K. Bakshi, A. Bakshi, and U. Bakshi, *Antenna And Wave Propagation*. Technical Publications, 2009.

[17] J. Moré, "The Levenberg-Marquardt algorithm: Implementation and theory," in *Numerical Analysis*, ser. Lecture Notes in Mathematics, G. Watson, Ed. Springer Berlin / Heidelberg, 1978, vol. 630, pp. 105–116.

[18] D. Gruyer, S. Demmel, B. D'Andrea-Novel, A. Lambert, and A. Rakotonirainy, "Simulation architecture for the design of cooperative collision warning systems," in *IEEE Intelligent Transportation Systems Conference*, 2012.